THEORY OF DISPERSION IN LOSSLESS MULTIMODE OPTICAL FIBRES

J.P. DAKIN, W.A. GAMBLING, H. MATSUMURA, D.N. PAYNE and H.R.D. SUNAK
Department of Electronics, University of Southampton, UK

Received 27 November 1972

Using the ray propagation model generalized expressions for the impulse response of multimode fibres have been derived. The analysis has been applied to lossless fibres for pulses having both gaussian and lambertian spatial distributions as well as impulse and gaussian temporal distributions. Detailed results are given for output pulse shapes and fibre dispersions for various configurations.

1. Introduction

Cladded multimode fibres, as well as graded-index fibres, are now serious competitors with single-mode fibres as potential long-distance transmission lines since low attenuations have been achieved [1–4], and the problems of launching and jointing are greatly eased because of the much larger (> 1000 times) light-carrying area. Furthermore by suitable design [5] multimode fibres can be made capable of exhibiting bandwidths approaching 1 GHz/km which are close to those expected, but no yet demonstrated, for single-mode fibres. Graded-index fibres also have large bandwidths [6] but have not yet been made with sufficiently low loss. Analyses of propagation in single-mode [7] and graded-index [8] fibres have been published and while the results of an analysis of a multimode fibre for the particular case of an input beam with both a spatial and a temporal gaussian dependence have appeared [9], the analysis itself was not described. We present here a generalized theory of propagation in multimode fibres based on a ray model. The results have been extended to include not only the earlier case [9] of a gaussian beam, such as that produced by a single-transverse-mode laser, but also to a lambertian spatial distribution, which is more typical of light-emitting diodes, and to both delta function and gaussian temporal dependences. The analysis is applicable to fibres having low-loss core and cladding and predicts values for dispersion close to those measured. The maximum pulse rates obtainable in such fibres is predicted for various experimental parameters and types of source.

2. Generalized analysis

In the ray propagation model a ray launched into the cylindrical core of an optical fibre at an angle θ to the axis is assumed to propagate, with unchanged angle, by successive reflections at the core/cladding interface, providing that it falls within the numerical aperture of the fibre. The propagation time of the ray in a fibre of length L depends on the angle θ and is given by

$$t(\theta) = \frac{n_1 L}{c \cos\theta} \quad \text{for } \theta \leqslant \tfrac{1}{2}\pi - \sin^{-1}(n_2/n_1), \qquad (1)$$

where n_1, n_2 are the refractive indices of the core, cladding, respectively. Energy launched into the fibre at large angles experiences a greater delay than that propagating at smaller angles thus giving rise to dispersion. Once the distribution of energy within the fibre is known a propagation time may be assigned to the rays and the output pulse shape is obtained by summing (i) over all rays propagating at angle θ, (ii) for all values of θ.

The energy distribution may be expressed in terms

of the angular flux density $I(\theta)$ in joule/steradian along a ray at angle θ. However for a radially symmetric distribution launched axially into a fibre all those rays comprising the hollow cone of semi-angle θ suffer the same propagation delay $t(\theta)$ and correspond to the same angular flux density $I(\theta)$. Thus in order to determine the output pulse shape from the fibre it is necessary to evaluate the energy distribution $\delta E = E(\theta)\delta\theta$ contained in the hollow annular cone laying between the angles θ and $\theta + \delta\theta$. This is simple since δE is given by the solid angle times the angular flux density $I(\theta)$ along a single ray, thus

$$\delta E = E(\theta)\delta\theta = 2\pi I(\theta)\sin\theta\ \delta\theta. \tag{2}$$

Furthermore if a delta function impulse of energy E_0 is launched at time $t = 0$ then

$$E_0 = \int_0^{\pi/2} E(\theta)\,\mathrm{d}\theta. \tag{3}$$

Now the energy δE launched in the hollow annular cone bounded by the angles θ, $\theta + \delta\theta$ arrives at the output in the time interval δt between $t(\theta)$ and $t(\theta + \delta\theta) = t + \delta t$. Furthermore if no mode conversion occurs then each value of t corresponds unambiguously to a corresponding value of θ given by eq. (1). Thus if $T(\theta)$ is a ray transmission factor then the power $P_0(\theta)$ arriving at the detector during the time interval $t(\theta + \delta\theta) - t(\theta)$ is

$$P_0(\theta) = \lim_{\delta\theta\to 0} \frac{E(\theta)T(\theta)\ \delta\theta}{t(\theta + \delta\theta) - t(\theta)}$$

$$= E(\theta)T(\theta)/(\mathrm{d}t/\mathrm{d}\theta) \tag{4}$$

and from eq. (1)

$$P_0(t) = \frac{c}{n_1 L} E\,[\theta(t)]\ T\,[\theta(t)]\ \frac{\cos^2\theta(t)}{\sin\theta(t)}, \tag{5}$$

where

$$\theta(t) = \cos^{-1}(n_1 L/ct).$$

Alternatively, in terms of $I(\theta)$ from eq. (2), we may write

$$P_0(t) = \frac{2\pi c}{n_1 L} I\,[\theta(t)]\ T[\theta(t)]\ \cos^2\theta(t) \qquad \text{for } n_1^2 L/cn_2 \geqslant t \geqslant n_1 L/c, \tag{6}$$

$$= 0 \qquad \text{for } t < n_1 L/c.$$

Eqs. (5) and (6) are quite general and can be used to find the impulse response for any form of symmetrical angular energy distribution. We shall illustrate its application to two typical forms of radiation flux, namely gaussian and lambertian.

3. Impulse response for a gaussian source

When a gaussian beam is launched into a fibre the beam waist is normally located centrally at the input face and spreads inside the fibre into a far-field pattern comprising effectively a linear cone of semi-angle $\theta_0 = \lambda/\pi\omega_0$ where ω_0 is the spot size (i.e., radius where the intensity has fallen to e^{-2} times that at the centre) at the beam waist. At a distance z along the fibre the energy flow per unit area through a transverse cross section is given by

$$I'(r, \phi, z) = (2I_0/\pi\omega^2)\exp(-2r^2/\omega^2), \tag{7}$$

where $\omega \approx \lambda z/\pi\omega_0$ is the spot size at z.

As before, the output pulse (temporal) shape is determined by the angular distribution $E(\theta)$ in the core and the energy passing through an annular ring between r and $r + \mathrm{d}r$ is

$$I(r)\mathrm{d}r = (4I_0/\omega^2)r\exp(-2r^2/\omega^2)\mathrm{d}r = E(\theta)\mathrm{d}\theta. \tag{8}$$

Now

$$z = \omega/\tan\theta_0 = r/\tan\theta \tag{9}$$

$$\therefore\ \mathrm{d}r/\mathrm{d}\theta = (\omega/\tan\theta_0)\sec^2\theta. \tag{10}$$

Thus

$$E(\theta) = \frac{4I_0\tan\theta}{\tan^2\theta_0\cos^2\theta}\exp\left(-\frac{2\tan^2\theta}{\tan^2\theta_0}\right) \tag{11}$$

Substituting (11) into (5) gives

$$P_0(t) = (2c/n_1 L\tan\theta_0)^2\, t \times \exp\left[-\frac{2}{\tan^2\theta_0}\left\{\left(\frac{ct}{n_1 L}\right)^2 - 1\right\}\right] T[\theta(t)] \quad \text{for } n_1 L/c \leqslant t \leqslant n_1^2 L/cn_2,$$

$$= 0 \quad \text{for } t < n_1 L/c. \qquad (12)$$

Eq. (12) shows that in a lossless fibre for which $T[\theta(t)] = 1$ the pulse shape depends on the length and refractive index of the core and on the angular width of the launched beam. The generalized shape of the output pulse is shown in fig. 1. The leading edge appears at time $t_1 = n_1 L/c$ and is of amplitude $P_0(t_1) = (4c/n_1 L\tan^2\theta_0)$, followed by a maximum at $t_m = (n_1 L\tan\theta_0/2c)$ of height $P_0(t_m) = (2c/n_1 L\tan\theta_0) \times \exp[(2\tan^{-2}\theta_0) - \frac{1}{2}]$. The output pulse ends after time $t_2 = n_1^2 L/n_2 c$.

The impulse response of a 1 km length of fibre with $n_1 = 1.551$ is shown in fig. 2a for various angular widths of input beam. The pulses shown are normalized to the same peak amplitude but, since the area under each curve corresponds to the same total energy E_0, it is obvious that the actual pulse height falls with increasing angular width. It may be seen that in this case the parameters are such that $t_1 > t_m$ and a maximum is not therefore observed. Thus propagation, and consequent dispersion, appreciably affects only the trailing side of the pulse and does not lengthen the leading edge. The final step is small and occurs at a time greater than those shown on the scale. For the same fibre length of 1 km the variation of dispersion with input angular width given in fig. 2b shows that if mode conversion can be avoided a maximum pulse rate of 500 MBit/sec (2 nsec/km) can be approached with a beam width of ± 2° falling to 20 MBit/sec (50 psec/m) at ± 13°. The analysis further shows that the pulse dispersion is approximately a linear function of length. Pulse dispersion is defined here as the difference in widths of the output and input pulses at half maximum intensity; for a delta function of course the width is zero.

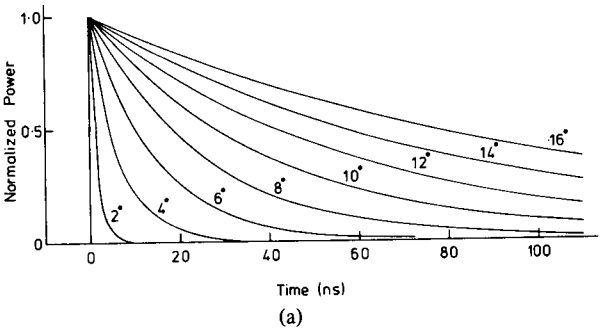

(a)

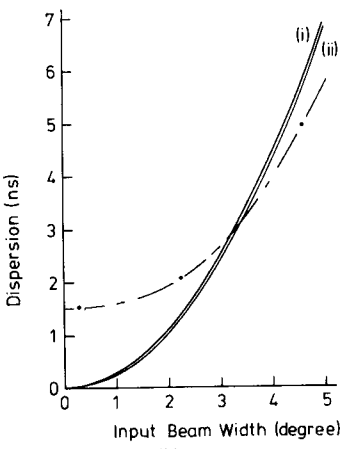

(b)

Fig. 2. (a) Normalized impulse response of 1 km length of fibre for the input angular beam widths in the cone shown on the curves. The fibre parameters are $n_1 = 1.551$, $n_2 = 1.485$. (b) Dispersion in 1 km of fibre for pulses having (i) delta function, (ii) 0.65 nsec gaussian, temporal distributions and a gaussian spatial distribution as a function of input beam angular width in the core. The dashed line shows experimental results for a liquid-core fibre with 0.97 m radius of curvature.

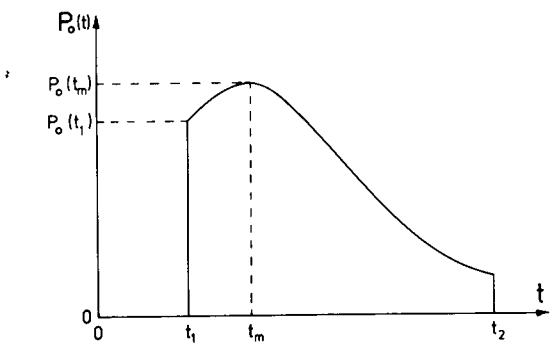

Fig. 1. Generalized impulse response for a source with a gaussian spatial distribution, as given by eq. (12). See text for explanation of symbols.

4. Impulse response for a lambertian source

The above results refer to a gaussian angular distribution such as would be produced by a single-transverse-mode laser. A light-emitting diode or other non-lasing source, on the other hand, produces a distribution which is more nearly lambertian, for which

$$I(\theta) = \pi^{-1}\cos\theta. \tag{13}$$

Substitution into eq. (6) gives the impulse response as

$$P_0(t) = (n_1 L/c)^2/t^3 \qquad \text{for } n_1 L/c \leqslant t \leqslant n_1^2 L/cn_2,$$
$$= 0 \qquad \text{for } t < n_1 L/c. \tag{14}$$

With a lambertian source the angular distribution of rays accepted by the fibre depends only on the numerical aperture and the effect of this parameter on the impulse response is plotted in fig. 3 for various values of core refractive index. The horizontal portion of the curves arises from the definition of dispersion as the width of the output pulse at half-maximum. Thus if the numerical aperture is increased past the value where the pulse amplitude at t_2 (cf., fig. 1) falls below half-maximum then further increase in NA lengthens the tail of the pulse but does not change the width at half-maximum. It should be noted further that with a lambertian source the numerical aperture also determines the launching efficiency. It may be seen that in the absence of any mode filtering mechanism the limiting pulse rate is, as expected, less than for a gaussian beam, and corresponds to 100MBit/sec (10 nsec/km) for NA = 0.1 falling to ≈ 2MBit/sec (600 nsec/km) for NA = 0.7. The relative launching efficiencies in the two cases are 1% and 50%. This result shows clearly, therefore, that with an LED source a careful optimization of the numerical aperture is necessary to achieve the desired compromise between bandwidth and launching efficiency.

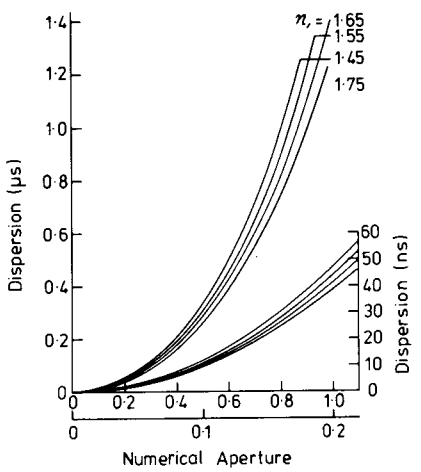

Fig. 3. Dispersion in a 1 km fibre for a lambertian source as a function of numerical aperture for the core refractive indices shown. The lower set of curves are for the lower and right-hand scales and for the same refractive indices as the upper one.

5. Gaussian temporal and spatial distribution

Having obtained an expression for the response of a fibre to a delta function impulse it is possible to obtain the shape of the output pulse for any input pulse by integration over the appropriate set of impulse functions. However the pulses produced by a mode-locked laser have an approximately gaussian temporal, as well as spatial, form and in this case an analytical solution is possible. Thus the shape of the input pulse to the fibre may be written:

$$G_i(t) = G_1 \exp(-2t^2/a^2), \tag{15}$$

where

$$\int_{-\infty}^{\infty} G_i(t)\mathrm{d}t = E_0.$$

Thus by convolution the output pulse shape for a gaussian-shaped input is given by

$$G_0(t) = \int_{\tau_1}^{\tau_2} P_0(t-\tau)G_i(\tau)\mathrm{d}\tau, \tag{16}$$

where

$$\tau_1 = t - (n_1^2 L/n_2 c), \qquad \tau_2 = t - (n_1 L/c).$$

Then substituting eqs. (12) and (15) into (16) we obtain

$$G_0(t) = 2\alpha \exp[\alpha(1-2t^2/a^2\beta^2\gamma)] \times \int_1^{n_1/n_2} x \exp[-\gamma(\beta x - 2t^2/a^2\gamma)]\, T[\theta(n_1 Lx/c)]\mathrm{d}x, \tag{17}$$

where $\alpha = 2/\tan^2\theta_0$, $\beta = n_1 L/c$, $\gamma = \alpha/\beta^2 + 2/a^2$.

Eq. (17) is now in a form suitable for computation and has been evaluated for a range of values of the parameters. For the lossless case, as before, $T[\ ] \equiv 1$.

Detailed computations have been made, and discussed elsewhere [9], for a specific length and type of fibre, namely 43 m of multimode fibre with a core of F7 glass ($n_d = 1.625$). The results given by eq. (17) are shown to be in reasonable agreement with those obtained by experiment for conditions where the effects of mode conversion are not large. For this comparatively short length the effect of the relatively high cladding loss is also small. Computations have also been made by representing the input gaussian pulse with a set of delta functions of appropriate amplitudes using eq. (12) and the results were the same as those obtained directly from eq. (17).

When pulse shapes were obtained from eq. (17) for a fibre ($n_1 = 1.551$) of length 1 km and an input pulse half-width of 0.65 nsec they were almost identical with those shown in fig. 2a and are not therefore given here. The only appreciable difference is that the leading edge of the gaussian input pulse has to be inserted. As shown in fig. 2b the pulse dispersion is also nearly unchanged. The earlier results are thus confirmed that the broadening in multimode fibres occurs almost entirely on the lagging edge and a measurement of full pulse width is necessary for a proper measurement of dispersion.

The analysis further shows that the calculated dispersion on a nanosecond time scale is not a strong function of pulse width. For example if the input is increased from 0 (impulse function) to 1 nsec the dispersion in a $\pm 2^\circ$ beam over a 1 km length falls from 1.1 to 1.0 nsec.

6. Conclusions

Generalized expressions for the impulse response of a multimode fibre have been derived. From these, output pulse shapes and dispersions for a lossless fibre, with input pulses having gaussian and lambertian spatial distributions, as well as impulse and gaussian temporal forms, have been obtained. The assumptions made are that the input beam is radially symmetric and is launched axially, and that there are no effects due to mode conversion or mode filtering. Our analysis differs from that of Gloge et al. [10] who take a more simplified approach. They appear to substitute eq. (1) into eq. (7) in order to obtain the response to a gaussian pulse.

In other work Gloge et al. [11], from measurements of frequency response of a fibre, suggest that the impulse response is of rectangular shape although they state that their results are also compatible with a rectangle having a sloping crest. Figs. 1 and 2a show that the impulse response of a lossless fibre is not of rectangular form and has approximately a sloping characteristic but that the exact form of the response depends very much on the experimental parameters.

The theoretical predictions given here may be applied to fibres made of low-loss core and cladding materials and the maximum bandwidths to be expected may be found from the dispersions given in the various figures. In practice mode conversion will constitute a limiting factor as shown by the experimental curve for a liquid-core fibre in fig. 2b. The measured dispersion has been extrapolated to a length of 1 km. The fibre was coiled on a drum of radius 0.97 m and as shown elsewhere [5] the curvature produces mode conversion and thus increased dispersion particularly at small angular beam width. It will be observed however that at larger widths the measured dispersion is less than that calculated. This is due to a mode filtering action caused by the high-loss cladding and a theoretical analysis of dispersion in fibres having both core and cladding loss will be published shortly.

References

[1] G.J. Ogilvie, Institute of Physics Meeting on Fibre Optical Communications, London (1972); Electron. Letters 8 (1972) 533.
[2] J. Stone, Appl. Phys. Letters 20 (1972) 239.
[3] D.N. Payne and W.A. Gambling, Electron. Letters 8 (1972) 374.
[4] R.D. Maurer, Paper presented at 1st European Electro-Optics Conference, Geneva (1972).
[5] W.A. Gambling, D.N. Payne and H. Matsumura, Opt. Commun. 6 (1972) 317.
[6] R. Bouillie and J.R. Andrews, Electron. Letters 8 (1972) 309.
[7] F.P. Kapron and D.B. Keck, Appl. Opt. 10 (1971) 1519.
[8] S. Kawakami and J. Nishizawa, IEEE Trans. Microwave Theory Tech. MTT-16 (1968) 814.
[9] W.A. Gambling, J.P. Dakin, D.N. Payne and H.R.D. Sunak, Electron. Letters 8 (1972) 260.
[10] D. Gloge, E.L. Chinnock, R.D. Standley and W.S. Holden, Electron. Letters 8 (1972) 527.
[11] D. Gloge, E.L. Chinnock and D.H. Ring, Appl. Opt. 11 (1972) 1534.